

## PROOF COVER SHEET

---

Journal acronym: RSPB

Author(s): Ki Hoon Han, Christopher Como, Jemin Kim, Sangwoo Lee,  
Jaewoong Kim, Dae Kyoo Kim and Young-Hoo Kwon

Article title: Effects of the golfer–ground interaction on clubhead speed in skilled  
male golfers

Article no: 1586983

Enclosures: 1) Query sheet  
2) Article proofs

---

Dear Author,

**1. Please check these proofs carefully.** It is the responsibility of the corresponding author to check these and approve or amend them. A second proof is not normally provided. Taylor & Francis cannot be held responsible for uncorrected errors, even if introduced during the production process. Once your corrections have been added to the article, it will be considered ready for publication.

Please limit changes at this stage to the correction of errors. You should not make trivial changes, improve prose style, add new material, or delete existing material at this stage. You may be charged if your corrections are excessive (we would not expect corrections to exceed 30 changes).

For detailed guidance on how to check your proofs, please paste this address into a new browser window: <http://journalauthors.tandf.co.uk/production/checkingproofs.asp>

Your PDF proof file has been enabled so that you can comment on the proof directly using Adobe Acrobat. If you wish to do this, please save the file to your hard disk first. For further information on marking corrections using Acrobat, please paste this address into a new browser window: <http://journalauthors.tandf.co.uk/production/acrobat.asp>

---

**2. Please review the table of contributors below and confirm that the first and last names are structured correctly and that the authors are listed in the correct order of contribution.** This check is to ensure that your name will appear correctly online and when the article is indexed.

Sequence	Prefix	Given name(s)	Surname	Suffix
1.		Ki Hoon	Han	
2.		Christopher	Como	
3.		Jemin	Kim	
4.		Sangwoo	Lee	
5.		Jaewoong	Kim	

6.		Dae Kyoo	Kim	
7.		Young-Hoo	Kwon	

PROOF ONLY

Queries are marked in the margins of the proofs, and you can also click the hyperlinks below.

Content changes made during copy-editing are shown as tracked changes. Inserted text is in **red font** and revisions have a red indicator ▲. Changes can also be viewed using the list comments function. To correct the proofs, you should insert or delete text following the instructions below, but **do not add comments to the existing tracked changes**.

## AUTHOR QUERIES

### General points:

1. **Permissions:** You have warranted that you have secured the necessary written permission from the appropriate copyright owner for the reproduction of any text, illustration, or other material in your article. Please see <http://journalauthors.tandf.co.uk/permissions/usingThirdPartyMaterial.asp>.
2. **Third-party content:** If there is third-party content in your article, please check that the rightsholder details for re-use are shown correctly.
3. **Affiliation:** The corresponding author is responsible for ensuring that address and email details are correct for all the co-authors. Affiliations given in the article should be the affiliation at the time the research was conducted. Please see <http://journalauthors.tandf.co.uk/preparation/writing.asp>.
4. **Funding:** Was your research for this article funded by a funding agency? If so, please insert 'This work was supported by <insert the name of the funding agency in full>', followed by the grant number in square brackets '[grant number xxxx]'.
5. **Supplemental data and underlying research materials:** Do you wish to include the location of the underlying research materials (e.g. data, samples or models) for your article? If so, please insert this sentence before the reference section: 'The underlying research materials for this article can be accessed at <full link> / description of location [author to complete]'. If your article includes supplemental data, the link will also be provided in this paragraph. See <http://journalauthors.tandf.co.uk/preparation/multimedia.asp> for further explanation of supplemental data and underlying research materials.
6. The **CrossRef database** ([www.crossref.org/](http://www.crossref.org/)) has been used to validate the references. Changes resulting from mismatches are tracked in **red font**.

**AQ1** The disclosure statement has been inserted. Please correct if this is inaccurate.

**AQ2** The CrossRef database ([www.crossref.org/](http://www.crossref.org/)) has been used to validate the references. Mismatches between the original manuscript and CrossRef are tracked in red font. Please provide a revision if the change is incorrect. Do not comment on correct changes.

**AQ3** Please provide missing DOI for reference "De Leva, 1996".

**AQ4** Please provide missing DOI for reference "Okuda et al., 2010".

**AQ5** Please provide missing DOI for reference "Williams, 2004".

- AQ6** Please provide missing DOI for reference "Worsfold et al., 2007".
- AQ7** Please provide missing DOI for reference "Worsfold et al., 2008".
- AQ8** Please provide missing DOI for reference "Worsfold et al., 2009".
- AQ9** Please provide missing publisher location for reference "Zatsiorsky and Seluyanov, 1983".

PROOF ONLY

## How to make corrections to your proofs using Adobe Acrobat/Reader

Taylor & Francis offers you a choice of options to help you make corrections to your proofs. Your PDF proof file has been enabled so that you can mark up the proof directly using Adobe Acrobat/Reader. This is the simplest and best way for you to ensure that your corrections will be incorporated. If you wish to do this, please follow these instructions:

1. Save the file to your hard disk.
2. Check which version of Adobe Acrobat/Reader you have on your computer. You can do this by clicking on the "Help" tab, and then "About".

If Adobe Reader is not installed, you can get the latest version free from <http://get.adobe.com/reader/>.

3. If you have Adobe Acrobat/Reader 10 or a later version, click on the "Comment" link at the right-hand side to view the Comments pane.

4. You can then select any text and mark it up for deletion or replacement, or insert new text as needed. Please note that these will clearly be displayed in the Comments pane and secondary annotation is not needed to draw attention to your corrections. If you need to include new sections of text, it is also possible to add a comment to the proofs. To do this, use the Sticky Note tool in the task bar. Please also see our FAQs here: <http://journalauthors.tandf.co.uk/production/index.asp>.

5. Make sure that you save the file when you close the document before uploading it to CATS using the "Upload File" button on the online correction form. If you have more than one file, please zip them together and then upload the zip file.

If you prefer, you can make your corrections using the CATS online correction form.

### Troubleshooting

**Acrobat help:** <http://helpx.adobe.com/acrobat.html>

**Reader help:** <http://helpx.adobe.com/reader.html>

Please note that full user guides for earlier versions of these programs are available from the Adobe Help pages by clicking on the link "Previous versions" under the "Help and tutorials" heading from the relevant link above. Commenting functionality is available from Adobe Reader 8.0 onwards and from Adobe Acrobat 7.0 onwards.

**Firefox users:** Firefox's inbuilt PDF Viewer is set to the default; please see the following for instructions on how to use this and download the PDF to your hard drive: [http://support.mozilla.org/en-US/kb/view-pdf-files-firefox-without-downloading-them#w\\_using-a-pdf-reader-plugin](http://support.mozilla.org/en-US/kb/view-pdf-files-firefox-without-downloading-them#w_using-a-pdf-reader-plugin)

## ARTICLE



# Effects of the golfer–ground interaction on clubhead speed in skilled male golfers

Ki Hoon Han, Christopher Como, Jemin Kim, Sangwoo Lee, Jaewoong Kim,  
Dae Kyoo Kim and Young-Hoo Kwon

5

Biomechanics Laboratory, Texas Woman's University, Denton, TX, USA

## ABSTRACT

The purposes of this study were to characterise the golfer–ground interactions during the swing and to identify meaningful associations between the golfer–ground interaction force/moment parameters and the maximum clubhead speed in 63 highly skilled male golfers (handicap  $\leq 3$ ). Golfers performed shots in 3 club conditions (driver, 5-iron and pitching wedge) which were captured by an optical motion capture system and 2 force plates. In addition to the ground reaction forces (GRFs), 3 different golfer–ground interaction moments (GRF moments, pivoting moments and foot contact moments) were computed. The GRF moment about the forward/backward (F/B) axis and the pivoting moment about the vertical axis were identified as the primary moments. Significant ( $p < 0.05$ ) correlations of peak force parameters (all components in the lead foot and F/B component in the trail foot) and peak moment parameters (lead-foot GRF moment and trail-foot pivoting moment) to clubhead speed were found. The lead-foot was responsible for generating the GRF moment, while the trail foot contributed to the pivoting moment more. The instant the lead arm becomes parallel to the ground was identified as the point of maximum angular effort, and the loading onto the lead-foot near this point was critical in generating both peak moments.

## ARTICLE HISTORY

Received 8 October 2018  
Accepted 18 February 2019

## KEYWORDS

Foot–ground interaction;  
ground reaction force;  
ground reaction moment;  
centre of pressure;  
moment arm

10

15

20

25

## Introduction

30

Two fundamental elements of high performance in golf are accuracy and consistency in shot direction and distance (Kwon, Como, Han, Lee, & Singhal, 2012). The shot distance, however, becomes increasingly important as the level of competitiveness increases (Hellstrom, 2009). Since the clubhead speed at impact is a key contributor to the initial ball speed and the overall shot distance (Hay, 1993, p. 282), it is crucial to be able to generate a high clubhead speed using the linear and angular motions of the body/club during the downswing. External forces and moments acting on the golfer's body during the swing cause linear and angular accelerations of the body-club system.

35

Two factors are of primary importance in clubhead speed development: (1) generation of large momentums of the body early in the downswing and (2) transfer of these generated momentums from the central segments (i.e., pelvis and thorax) to the peripheral segments (i.e., arms and club). With air resistance ignored, the ground reaction forces (GRFs; the reaction forces caused by the push against the ground) and the ground reaction moments (GRMs; the reaction moments about the vertical axis produced by the twisting interactions between the shoe and the ground at the shoe/turf interface) acting on the golfer's feet are the only external forces/moments that can alter the momentums of the golfer-club system. Internal forces/moments acting between the body parts (including the club) cause momentum transfers within the system.

Several golf studies have focused on the foot-ground interaction measures, such as GRF, GRM and centre of pressure (CP; GRF's point of action about which the moments about the horizontal axes are balanced), as well as the clubhead/ball speed (Barrentine, Fleisig, Johnson, & Woolley, 1994; Ball & Best, 2007a, 2007b; Chu, Sell, & Lephart, 2010; Okuda, Gribble, & Armstrong, 2010; Robinson, 1994; Williams, 2004; Worsfold, Smith, & Dyson, 2007, 2008, 2009). In a study comparing peak GRFs, peak GRMs and CP ranges among skill groups, Barrentine et al. (1994) reported significant correlations between select GRF, and GRM parameters and clubhead speed. Williams (2004) compared peak horizontal GRFs and select CP parameters among handicap groups, and reported significant correlations between handicap and clubhead speed. Based on CP excursion patterns, Ball and Best (2007a, 2007b) identified large clusters: a 'Reverse' group and a 'Front Foot' group. While clubhead speed was not different between these clusters, significant partial correlations between clubhead speed and select CP parameters in each cluster (peak velocity and excursion range in the Front Foot group and positions and velocities at various swing events in the Reverse group) were found.

In an effort to develop a set of ball speed prediction equations, Chu et al. (2010) measured vertical GRFs of the feet, along with a group of kinematic variables, at different events (i.e., top, acceleration, 40 ms prior to impact and impact) and reported a prediction model that included the vertical GRF parameters of the 'acceleration' and '-40 ms' events. Okuda et al. (2010) compared vertical GRFs at different swing events and maximum vertical GRFs between skill groups (i.e., skilled and low skilled). Worsfold et al. (2007, 2008, 2009) measured vertical GRFs and GRMs, and compared the shoe-ground interaction characteristics among different outer sole designs (i.e., metal spikes, alternative spikes and flat-soled).

One area that has not received much attention in the previous studies is the angular 'golfer-ground' interaction (i.e., the global effect of the foot-ground interaction on the angular motion of the golfer-club system). Two sources of external moments accelerate the golfer-club system angularly (Figure 1): (1) the moments generated by the GRFs about the system's centre of mass (CM) and (2) the GRMs directly acting on the feet:

$$\mathbf{M} = \sum_i (\mathbf{r}_i \times \mathbf{F}_i + \boldsymbol{\tau}_i) \quad (1)$$

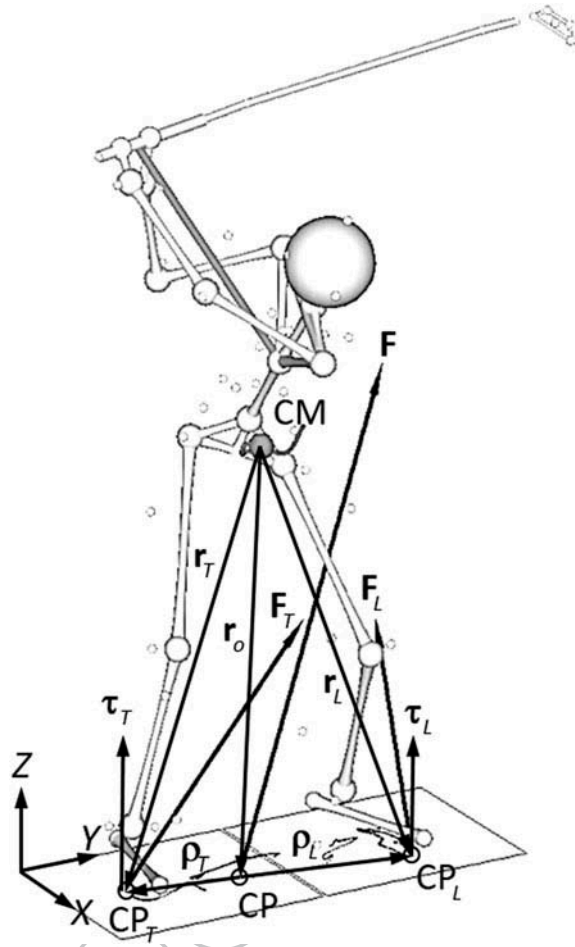


**Figure 1.** The external forces and moments acting on the golfer-club system during the swing.  $F_L$  &  $F_T$  are the ground reaction forces (GRF) acting on the lead foot and the trail foot, respectively,  $\tau_L$  &  $\tau_T$  are the ground reaction moments about the vertical axis,  $r_L$  &  $r_T$  are the relative positions of the foot centres of pressure (CP) to the body-club system centre of mass (CM),  $\rho_L$  &  $\rho_T$  are the relative positions of the foot CPs to the combined CP.  $r_o$  is the relative position of the combined CP to the CM, and  $F$  is the combined GRF.

where  $M$  is the total external moment acting on the golfer-club system about its CM,  $r_i$  is the relative position of a foot CP to the CM,  $F_i$  is the GRF acting on a foot, and  $\tau_i$  is the GRM acting on a foot. Although GRFs, CPs and GRMs are all involved in Equation (1), considering these factors on their own does not provide a holistic assessment of the golfer-ground interaction (e.g., Barrentine et al., 1994; Robinson, 1994) since: (1) the relative position and orientation of the GRF vector to the CM can alter the moment generated by the GRF substantially, and (2) it is not possible to inspect various moment generation mechanisms and the relative magnitudes of the moments produced by these mechanisms. Moreover, several investigators considered only the vertical GRFs in establishing group differences and/or correlations (e.g., Chu et al., 2010; Okuda et al., 2010; Worsfold et al., 2007, 2008, 2009), while others focused on the combined CP

85

90



excursion as a measure of weight shift (Ball & Best, 2007a, 2007b). The magnitudes of the moments generated by the GRFs (the first term in Equation (1)) are dependent on the moment arms formed by GRF vectors against the CM and the moment arms in turn are sensitive to the inclinations of the GRF vectors (i.e., horizontal GRF components). The combined CP position is determined by the relative proportions of individual vertical GRFs and does not reflect the actual weight shift (CM motion) pattern. Therefore, the body/club motions and the foot-ground interaction must be considered collectively to develop a greater understanding of the golfer-ground interaction.

One common trend in golf biomechanics research is the inclusion of golfers of varying skill levels. As expected, significant inter-group differences in select foot-ground interaction measures and clubhead/ball speed have been reported (Barrentine et al., 1994; Okuda et al., 2010; Williams, 2004). Significant correlations between foot-ground interaction measures and clubhead (or ball) speed have also been reported (Chu et al., 2010; Robinson, 1994; Williams, 2004), but it is likely that these correlations were driven by the heterogeneity in the sample. The correlation profiles obtained from a large heterogeneous group may not be the same to those obtained from individual homogeneous subgroups. For this reason, Ball and Best (2007b) performed a cluster analysis first and then established correlation profiles within each large cluster. It is, therefore, necessary to use a relatively homogenous sample, such as highly skilled golfers, in understanding the direct interrelationships among various performance parameters.

Despite the importance of the golfer-ground interaction in the golf swing, only the direct outputs of the force plates (GRFs, CPs and GRMs) have been reported in previous studies. And the effects of these measures on the golfer's body and club motion are therefore not well understood. The purposes of this study were (1) to characterise the linear and angular golfer-ground interactions by establishing generalised patterns of various golfer-ground interaction forces and moments in a group of highly skilled golfers and (2) to identify meaningful associations between the golfer-ground interaction force and moment parameters and maximum clubhead speed. Three different golfer-ground interaction moments (GRF moments, pivoting moments and foot contact moments) were computed for the combined and individual feet (lead and trail), in addition to the GRFs. It was hypothesised that (1) peak golfer-ground interaction forces would reveal significant correlations to maximum clubhead speed, and (2) peak golfer-ground interaction moments would reveal significant correlations to maximum clubhead speed.

## Methods

### *Theoretical framework—breakdown of the foot-ground interaction moments*

With air resistance ignored,  $\beta$  groups of external moments act on the golfer-club system: the moments generated by the GRFs and the GRMs (Figure 1). The total external moment acting on the golfer-club system (Equation (1)) can then be further broken down to  $\beta$  terms:

$$\begin{aligned}
\mathbf{M} &= \sum_{i=1}^2 [(\mathbf{r}_o + \boldsymbol{\rho}_i) \times \mathbf{F}_i + \boldsymbol{\tau}_i] \\
&= \mathbf{r}_o \times \sum_{i=1}^2 \mathbf{F}_i + \sum_{i=1}^2 \boldsymbol{\rho}_i \times (\mathbf{F}_{xyi} + \mathbf{F}_{zi}) + \sum_{i=1}^2 \boldsymbol{\tau}_i \\
&= \mathbf{r}_o \times \mathbf{F} + \sum_{i=1}^2 \boldsymbol{\rho}_i \times \mathbf{F}_{xyi} + \sum_{i=1}^2 \boldsymbol{\tau}_i \\
&= \begin{bmatrix} d_x F_{yz} \\ d_y F_{zx} \\ d_z F_{xy} \end{bmatrix} + \begin{bmatrix} 0 \\ 0 \\ \sum_{i=1}^2 \rho_i F_{xyi} \end{bmatrix} + \begin{bmatrix} 0 \\ 0 \\ \sum_{i=1}^2 \tau_i \end{bmatrix} \quad (2)
\end{aligned}$$

since

$$\sum_{i=1}^2 \boldsymbol{\rho}_i \times \mathbf{F}_{zi} = 0 \quad (3)$$

where  $\mathbf{r}_o$  is the relative position of the combined CP to the system CM,  $\boldsymbol{\rho}_i$  is the relative position of a foot CP to the combined CP,  $\mathbf{F}_{xyi}$  is the horizontal GRF ( $= \mathbf{F}_{xi} + \mathbf{F}_{yi}$ ), and  $\mathbf{F}_{zi}$  is the vertical GRF. The  $x$ -axis and the  $y$ -axis of the reference frame correspond to the forward/backward (F/B) axis and the toward/away (T/A) axis, respectively (Figures 1 and 2).  $[F_{yz}, F_{zx}, F_{xy}]$  are the magnitudes of the combined GRF projected to the  $yz$ -plane,  $zx$ -plane

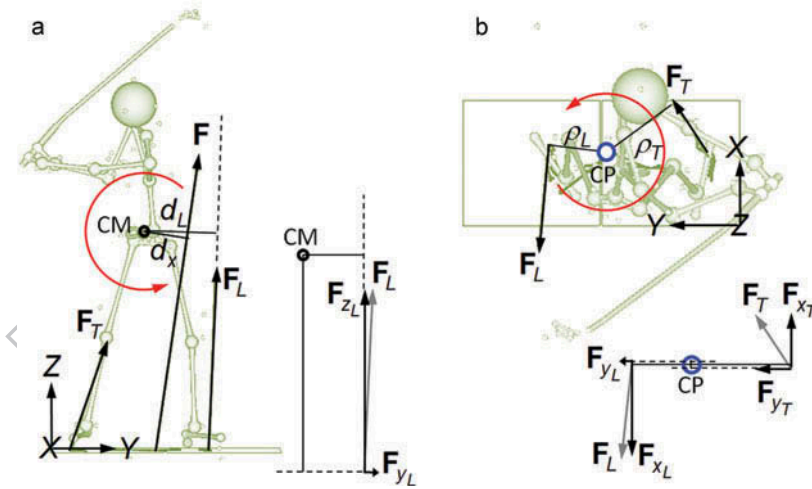


**Figure 2.** Key golfer-ground interaction moments: the ground reaction force (GRF) moments in the frontal plane (a) and the pivoting moments about the combined centre of pressure (CP) in the horizontal plane (b).  $\mathbf{F}$ ,  $\mathbf{F}_L$  and  $\mathbf{F}_T$  are the combined, lead-foot and trail-foot GRFs, respectively, and  $d_x$ ,  $d_L$  and  $d_T$  are the moment arms formed by the combined, lead-foot and trail-foot GRFs, respectively, either against the centre of mass (CM) (a) or the combined CP (b).  $d_L$  is the moment arm formed by the lead-foot GRF about the CM in the frontal plane. In both planes, a positive (counterclockwise) moment is in the downswing direction, promoting either acceleration of the downswing or deceleration of the backswing. GRF components ( $F_x$ ,  $F_y$ ,  $F_z$ ) and their respective moment arms against the CM and combined CP are also presented.

and  $xy$ -plane, respectively,  $F_{xy_i}$  is the magnitude of the  $xy$ -component of a foot GRF, and  $\tau_i$  is the vertical free moment acting on a foot.  $[d_x, d_y, d_z]$  are the moment arms formed by the combined GRF with respect to the system CM in the  $yz$ -,  $zx$ - and  $xy$ -plane, respectively, while  $\rho_i$  is the moment arm formed by a horizontal GRF with respect to the combined CP on the horizontal plane (Figure 2). The moment arms hold positive values if the resulting moments are counterclockwise, and vice versa. Equation (3) was derived from the definition of the combined CP.

Equation (2) can be rewritten as

$$\mathbf{M} = \mathbf{G} + \mathbf{P} + \mathbf{C} = \begin{bmatrix} G_x \\ G_y \\ G_z \end{bmatrix} + \begin{bmatrix} 0 \\ 0 \\ P_z \end{bmatrix} + \begin{bmatrix} 0 \\ 0 \\ C_z \end{bmatrix} \quad (4)$$

where  $\mathbf{G}$  is the GRF moment generated by the combined GRF about the golfer-body CM (Figure 2(a)),  $\mathbf{P}$  is the pivoting moment generated by the horizontal GRFs about the combined CP (Figure 2(b)), and  $\mathbf{C}$  is the foot contact moment acting directly on the feet. These  $\beta$  moment terms in Equation (4) represent different moment generation mechanisms. As shown in Equations (2) and (3), the horizontal moment components ( $G_x, G_y$ ) can be explained entirely by the GRF moment mechanism, but the vertical moment comes from all  $\beta$  mechanisms ( $G_z + P_z + C_z$ ).

## Participants

Sixty-three highly skilled male golfers (handicap  $\leq 3$ ), including touring professionals, elite amateur (collegiate) players and teaching professionals, participated in this study:  $M$  ( $\pm SD$ ) mass = 83.6 ( $\pm 8.8$ ) kg, height = 181.6 ( $\pm 5.7$ ) cm and age = 30.9 ( $\pm 8.6$ ) years. Participants were free of major injuries at the time of data collection which could potentially hinder their maximal effort swings. One golfer was left-handed. The research protocol was approved by the Institutional Review Board of Texas Woman's University and written informed consent was obtained from each participant prior to data collection.

## Club conditions

Three club conditions were used: driver, 5-iron and pitching wedge (Kwon et al., 2012). Participants used their own clubs. Five successful swing trials were captured per club condition. Success of a shot was judged based on the flight characteristics, such as direction and launch angle of the ball judged by the locations of impact on the front wall, and golfer's perceived solidness of ball striking. Foam balls were used instead of real balls in the indoor laboratory setting (Kwon et al., 2012; Kwon, Han, Como, Lee, & Singhal, 2013).

## Experimental set-up and data capture

The swing motion data and the GRF/GRM data were captured at 250 Hz by a 10-camera optical motion capture system (Mx T-10 series, VICON, Centennial, CO, USA) and  $2$  force plates (OR-6 series, AMTI, Watertown, MA, USA) in an indoor motion analysis facility (Figure 3). Cameras were calibrated before each data collection session following manufacturer's guidelines. Force plates were zeroed repeatedly at the beginning of each

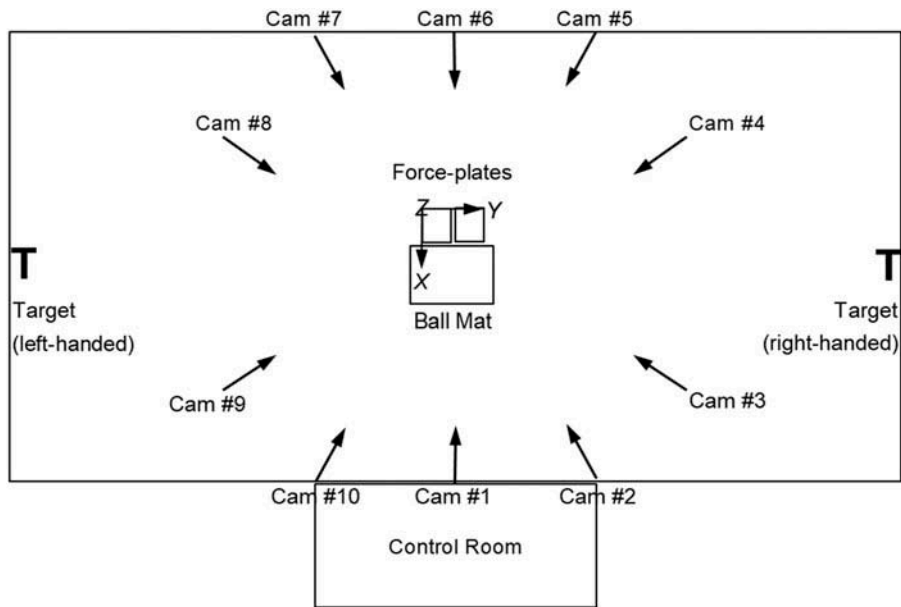


**Figure 3.** The experimental set-up used in this study. The  $x$ -,  $y$ - and  $z$ -axes of the global reference frame were aligned with the forward/backward, toward/away and vertical axes, respectively.

trial condition and after 3 trials were collected in a trial condition. The plate surfaces were covered with commercial golf practice mats (Hank Haney Profinity Practice Hitting Mat) to prevent slipping. Golfers wore their own golf shoes.

The 'TWUGolfer 3.0' marker set with 65 retro-reflective markers was used for motion capture (Kwon et al., 2012). Participants wore black spandex shorts only during the trials to minimise marker motion artefacts. A 'T-pose' static trial (with 49 markers on golfer's body) was first captured for each golfer. Two additional static trials were also captured for each club condition: club (11 markers; 5 club-head markers and 6 shaft markers) and ball mat (5 markers; 1 ball marker and 4 mat markers). A regular golf ball covered with retro-reflective tape was used in the ball-mat static trial. Swing trials were then captured with 15 static-only markers (10 body markers, 4 clubface markers and the ball) removed. In the swing trials, the ball covered with reflective tape was replaced with a foam ball. VICON Nexus (version 1.8) was used in trial capture and marker labelling.

Shots were made against a target marked on a wall (Figure 3). Target lines were also marked on the floor to guide the shots. The distance from the centre of the ball mat to the target was approximately 10.5 m. Golfers faced in the +X (forward) direction in the set-up position and made shots along the T/A axis in 2 different directions depending on their handedness: right-handed golfers in the +Y direction and left-handed golfers in the -Y direction (Figure 3). Participants reported no abnormal feel or alteration of swing motion due to the foam ball. Tees with various heights were used in the driver condition to accommodate each golfer's preferred tee height.

## Data reduction and processing

Captured trials containing both motion and force data stored in C3D files were imported into Kwon3D Motion Analysis Suite (version XP, Visol, Seoul, Korea) for subsequent data processing and analysis. The CP data from the force plates were transformed to the global laboratory reference frame coordinates. All data were then up-sampled to 1,000 Hz by a cubic spline-based routine for improved time resolution. The raw coordinates of the reflective markers were digitally filtered by a 4th-order zero phase-lag Butterworth low-pass filter (Winter, 2005, pp. 42–50), with different cut-off frequencies applied: 6 Hz for the body/ball-mat markers, 15 Hz for the proximal club markers and 30 Hz for the distal shaft/clubhead markers (Kwon et al., 2013).

A 107-point body model ("TWUGolfer 3.0") was used in data reduction and processing. In this model, a total of 32 secondary points (including clubface markers and ball marker) were computed based on the coordinates of related markers. Since the clubface markers were removed in the swing trials, the coordinates of these markers were computed indirectly by using a rigid body method (Kwon, 2008; Kwon et al., 2012; Williams & Sih, 2002). The relative positions of the clubface markers to non-collinear markers (2 markers on the distal shaft and 1 on the clubhead) were computed in the club static trial and applied in the swing trials. The clubhead point was then computed as the centroid of the clubface markers. The position of the ball was computed in a similar way, in that the relative positions of the ball to the mat markers were computed in the ball-mat static trial and applied in the swing trials.

Eighteen segments, including 3 trunk segments (thorax, abdomen and pelvis) and 2 club segments (shaft/grip and clubhead), were defined based on joint centres (ankles, knees, hips, wrists, elbows, shoulders, mid-shoulder, mid-trunk, mid-pelvis) and end points. The mid-shoulder point (mid-point of the suprasternal notch and the spinous process of the 7th cervical vertebra) represented the superior end of the thorax. The mid-trunk point (mid-point of the xyphoid process and the spinous process of the 12th thoracic vertebra) represented the joint linking the thorax and the abdomen. The mid-pelvis point (centroid of the ASIS [anterior superior iliac spine] and PSIS [posterior superior iliac spine] markers) represented the link between the abdomen and the pelvis. The positions of other joints and hand centres were computed following the methods outlined by Kwon et al. (2012). The body segment parameters (mass, CM and radius of gyration ratios) originally reported by Zatsiorsky and Seluyanov (1983) and corrected by De Leva (1996) were used in locating the segment CMs and the whole body CM. The CM of the golfer's body, not the golfer-club system, was used in the computation of the GRF moments for 2 reasons: (1) measuring the inertial properties of the club (clubhead and shaft/grip) accurately was cumbersome, and (2) the effect of the club on the computed GRF moment was negligible due to its relatively small mass (up to ~300 g). When both the golfer's body CM and the golfer-club system CM were calculated for a golfer (87 kg, 185 cm) before data collection began, the maximum difference observed in the peak GRF moments was approximately 0.63%.

A total of 11 swing events (Figure 4) were defined: BA (break-away), MB (mid backswing), LBA (late backswing, arm-based), LB (late backswing), EPR (end of pelvis

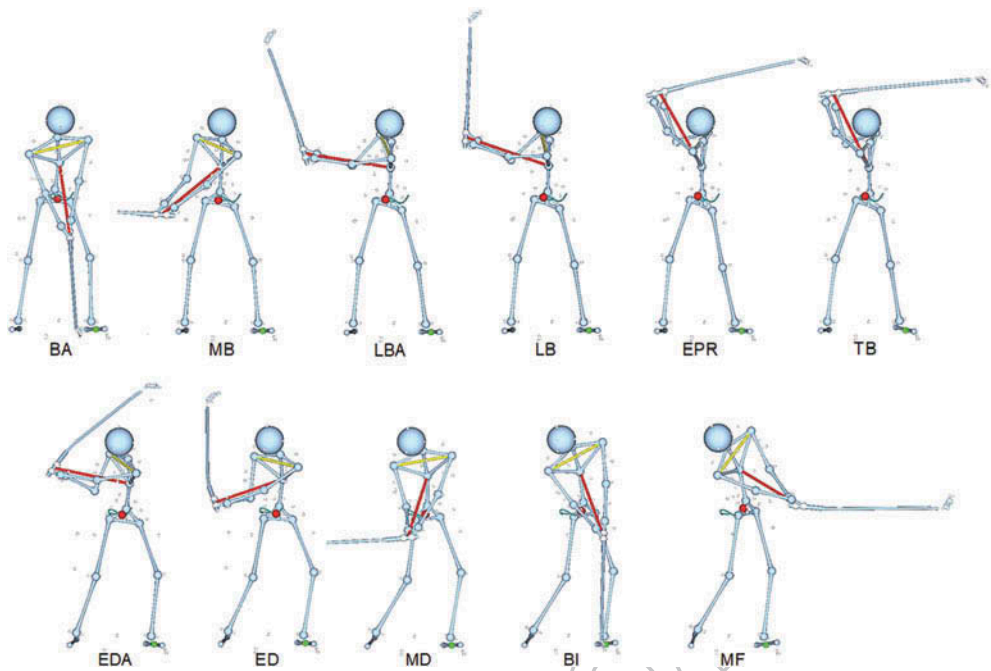


**Figure 4.** Swing events: BA: breakaway; MB: mid backswing; LBA: late backswing, arm-based; LB: late backswing; EPR: end of pelvis rotation; TB: top of backswing; EDA: early downswing, arm-based; ED: early downswing; MD: mid downswing; BI: ball impact; MF: mid follow-through. Among these, MB, LB, ED, MD and MF are based on the angular position (horizontal or vertical) of the club in the frontal (face-on) view, whereas LBA and EDA are lead arm-based (parallel to the ground). BA is the instant the clubhead moved by more than 2 cm from the initial position at address. EPR is when the pelvis reverses the direction of rotation near the end of backswing. TB is the instant the club changes the direction of rotation. BI is the instant the clubface makes contact with the ball.

rotation), TB (top of backswing), EDA (early downswing, arm-based), ED (early downswing), MD (mid downswing), BI (ball impact) and MF (mid follow-through).

### Variable computation

The clubhead speed was computed through a numerical differentiation of the unfiltered position data of the clubhead. The GRF moments produced by individual GRFs, as well as the combined GRF, the pivoting moments and the foot contact moment, were computed (Equations (2) and (4)). The clubhead speed was normalised to the golfer's body height (BH) and expressed in BH/s. The force and moment data were normalised to the golfer's body weight (BW) and expressed in BW and BW·cm, respectively.

Generalised patterns of the golfer-ground interaction forces and moments (Figures 5 and 6) were developed through ensemble averaging (BA to MF). A subphase-by-subphase time normalisation strategy was used, which included the following steps: (1) average individual subphase times were computed from all involved trials; (2) their relative proportions to the average whole phase (BA-MF) time were computed; (3) time normalisation was conducted subphase by subphase and the time points were reduced to 101 normalised time points (0–100%); (4) the



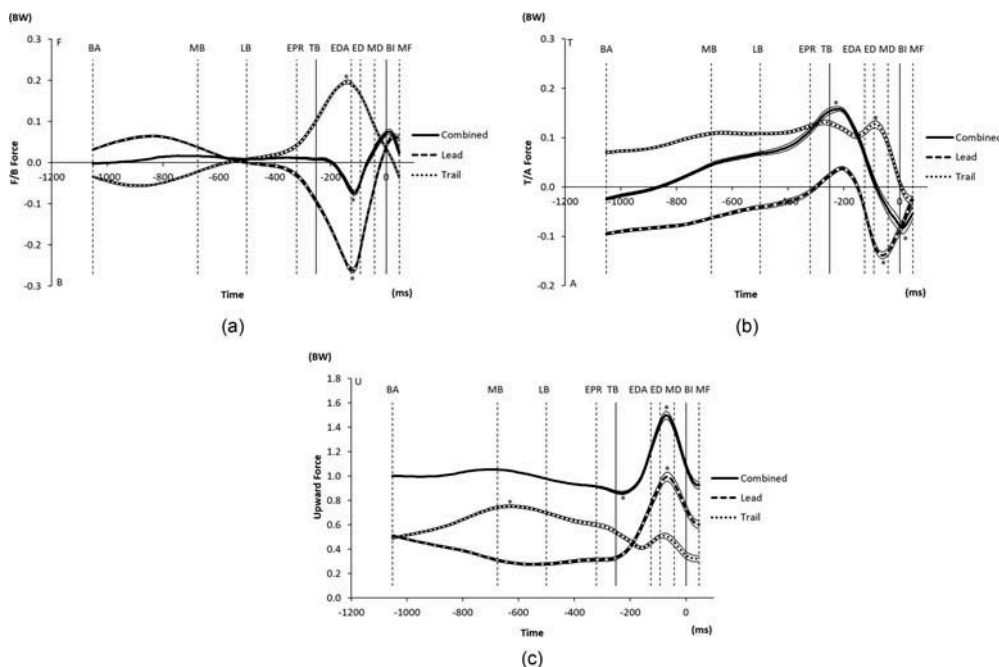


**Figure 5.** The ensemble-average patterns of the normalised ground reaction force (GRF) components (driver;  $n = 63$ ): forward/backward (a), toward/away (b) and upward (c). The thin black lines show the  $\pm$  SE patterns. F: forward; B: backward; T: toward; A: away; U: upward; BW: body weight. See Figure 3 for the event abbreviations. Peak forces used in the correlation analysis are marked with asterisks.

and standard error (SE) of all involved trials were computed at each normalised time point; (5) the average whole-phase time was applied to the ensemble average pattern to express the horizontal axis in actual time (in ms), with BI representing the zero-time event.

As there was 1 left-handed golfer among the participants, handedness-neutral terms were used in describing the following directions: (1) 'lead' ('left' for a right-handed golfer, but 'right' for a left-handed golfer) and 'trail' ('right' for a right-handed golfer, but 'left' for a left-handed golfer) were used in describing the sides; (2) 'towards' the target ('+Y' for a right-handed golfer and '-Y' for a left-handed golfer) and 'away' from the target ('-Y' for a right-handed golfer and '+Y' for a left-handed golfer) were used in describing the direction of the lateral force. Before ensemble averaging, appropriate directional multipliers ('+1' for the right-handed golfers and '-1' for the left-handed golfers) were applied to the F/B and vertical-axis moments and the T/A force.

Based on the ensemble-averaged force patterns, the following peak force parameters were recognised and used in the analysis:

- F/B component ( $F_x$ , Figure 5(a)): combined (+), lead-foot (-) and trail-foot (+)
- T/A component ( $F_y$ , Figure 5(b)): combined (both + and -), lead-foot (-) and trail-foot (+)

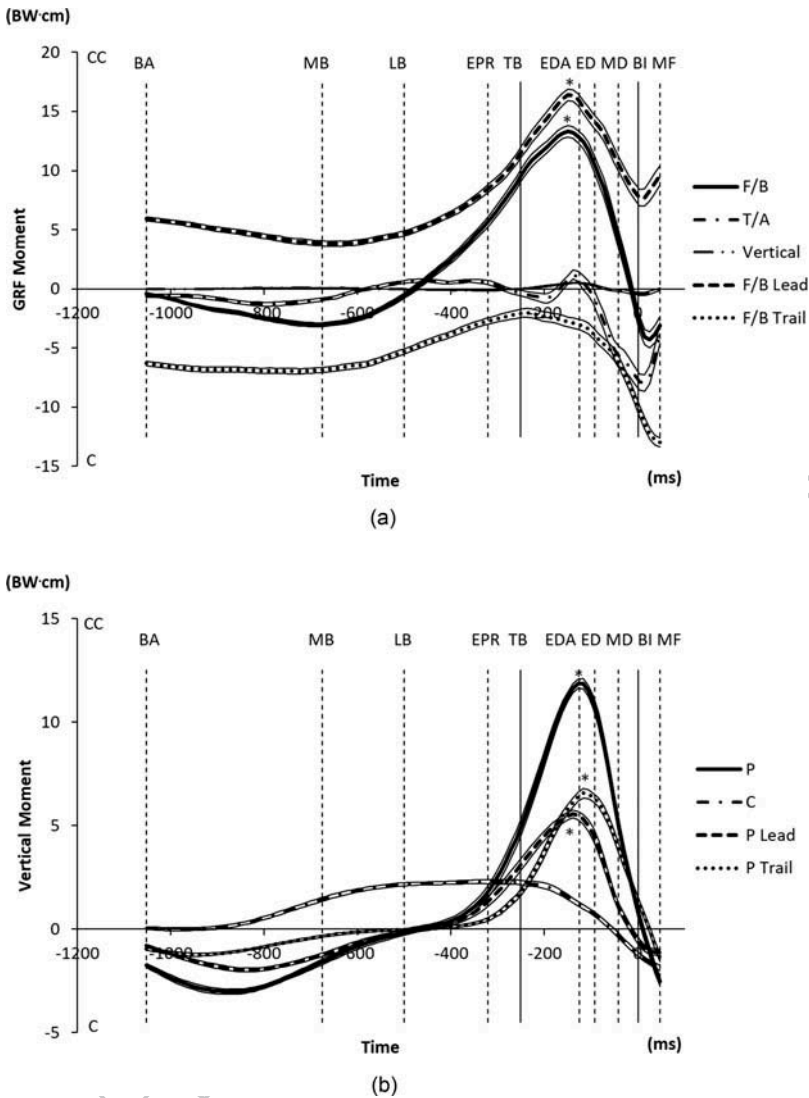


**Figure 6.** The ensemble-average patterns of the normalised golfer-ground interaction moments (driver;  $n = 63$ ): ground reaction force (GRF) moments (a) and vertical moments (b). The thin black lines show the  $M \pm SE$  patterns; F/B: forward/backward; T/A: toward/away; P: pivoting moment; C: foot contact moment; BW: body weight; CC: counterclockwise; C: clockwise. See Figure 3 for the event abbreviations. Peak moments used in the correlation analysis are marked with asterisks.

- Vertical component ( $F_z$ , Figure 5(c)): combined (+maximum and +minimum), lead-foot (+) and trail-foot (+)

280

Based on the moment patterns, the following peak moment parameters were also identified:

- GRF moment about the F/B axis ( $G_x$  in Figure 6(a)): combined (+) and lead-foot (+)
- Pivoting moment ( $P_z$  in Figure 6(b)): combined (+), lead-foot (+) and trail-foot (+)



Peak T/A and vertical GRF moments ( $G_y$  and  $G_z$ ) and foot contact moment ( $C_z$ ) were excluded from the analysis because either the peak value occurred late near the impact or the magnitude was small (Figure 6). The signs of the peak values reflect the directions of the 'reaction' force and moment components acting on the body.

### Statistical analysis

Average values of the 5 repeated trials were used in the statistical analysis. After outliers ( $|t| > 3.2$ ) were removed from the data set, normality test was conducted. Pearson product-moment correlation coefficients of peak normalised clubhead speed (BH/s) to peak normalised forces (BW) and moments (BW·cm) were computed in each club condition. To associate the force/moment 'magnitudes' to peak clubhead speed, the signs of the peak force/moment parameters were dropped before the correlation analysis. In the interpretation of the correlations,  $r = 0.1$ ,  $0.3$  and  $0.5$  were used as the thresholds for small, moderate and large correlations (Lee, 2016). Ninety-five per cent confidence interval (CI) of the normalised variables were computed. Statistical analyses were performed using IBM SPSS version 19 (IBM, New York, NY, USA) with an  $\alpha$ -level set at 0.05.

### Results

The  $M$  ( $\pm SD$ ) peak clubhead speeds were  $48.3 \pm 2.5$  m/s ( $26.6 \pm 1.4$  BH/s, 95% CI: 26.4–27.1 BH/s),  $41.3 \pm 1.93$  m/s ( $22.7 \pm 1.2$  BH/s, 95% CI: 22.6–23.1 BH/s) and  $37.5 \pm 1.9$  m/s ( $20.7 \pm 1.2$  BH/s, 95% CI: 20.5–21.1 BH/s) for the driver, 5-iron and pitching wedge conditions, respectively. The ensemble-average patterns of the golfer-ground interaction force and moment components obtained from the driver condition are presented in Figures 5 and 6. While the magnitudes were smaller, the other club conditions also revealed similar generalised patterns with slightly shorter overall swing times (driver =  $1,054 \pm 162$  ms, 5-iron =  $1,030 \pm 156$  ms and pitching wedge =  $1,016 \pm 134$  ms).

Outliers were identified in the driver condition (1 in trail-foot forward force and 2 in trail-foot toward force) and in the 5-iron condition (1 in trail-foot forward force and 1 in trail-foot upward force). All cases were associated with the trail foot and no outlier was observed in the moment parameters and in the clubhead speed. With outliers eliminated, all variables met the normality requirements.

Among the peak normalised force parameters, combined and lead-foot backward forces, trail-foot forward force, lead-foot away force, combined maximum and minimum upward forces and lead-foot upward force showed significant ( $p < 0.05$ ) correlations to peak clubhead speed in 2 or more club conditions (Table 1). Combined toward and away forces, trail-foot toward force and trail-foot upward force generally revealed insignificant correlations. Most of the significant correlations were moderate ( $0.3 \leq r < 0.5$ ), with some small ( $0.1 \leq r < 0.3$ ) and 1 large ( $0.5 < r$ ) correlation (lead-foot backward force).

Among the peak normalised moment parameters, combined and lead-foot GRF moments about the F/B axis and combined and trail-foot pivoting moments revealed significant correlations to peak normalised clubhead speed in 2 or more club



Table 1. Peak golfer–ground interaction forces (M ± SD [95% CI]) and their correlations to peak clubhead speed.

Variable	Foot	Club		
		Driver	5-Iron	Pitching wedge
Forward (+)/ Backward (-) (F <sub>x</sub> )	Combined (-)	84.8 ± 36.2 0.10 ± 0.05 [0.09, 0.12] r 0.317*	72.3 ± 32.9 0.09 ± 0.04 [0.08, 0.10] 0.218	61.2 ± 31.6 0.07 ± 0.04 [0.07, 0.08] 0.306*
	Lead (-)	229.8 ± 39.8 0.28 ± 0.05 [0.27, 0.29] r 0.458*	210.3 ± 39.1 0.26 ± 0.05 [0.24, 0.27] 0.444*	192.0 ± 39.6 0.24 ± 0.05 [0.22, 0.25] 0.554*
	Trail (+)	166.4 ± 25.8 0.21 ± 0.04 [0.20, 0.21] r 0.295* (n = 62)	154.4 ± 21.8 0.19 ± 0.03 [0.18, 0.20] 0.308* (n = 62)	147.1 ± 23.6 0.18 ± 0.03 [0.17, 0.19] 0.419*
	Combined (+)	166.4 ± 25.8 0.19 ± 0.05 [0.18, 0.20] r 0.073	154.6 ± 35.0 0.19 ± 0.03 [0.18, 0.20] 0.196	147.0 ± 33.1 0.18 ± 0.04 [0.17, 0.19] 0.350*
Toward (+)/ Away (-) (F <sub>y</sub> )	Combined (-)	108.0 ± 61.4 0.12 ± 0.08 [0.11, 0.15] r 0.061	111.3 ± 50.7 0.13 ± 0.06 [0.12, 0.15] -0.013	110.2 ± 42.3 0.13 ± 0.05 [0.12, 0.15] 0.201
	Lead (-)	144.0 ± 43.0 0.18 ± 0.05 [0.16, 0.19] r 0.447*	126.1 ± 36.7 0.15 ± 0.04 [0.14, 0.16] 0.253*	118.8 ± 32.4 0.14 ± 0.03 [0.14, 0.15] 0.249*
	Trail (+)	144.4 ± 34.6 0.18 ± 0.04 [0.17, 0.19] -0.050 (n = 61)	134.4 ± 28.9 0.17 ± 0.03 [0.16, 0.17] -0.031	126.6 ± 26.8 0.16 ± 0.03 [0.15, 0.16] 0.188
	Combined (max)	1,327.3 ± 216.4 1.62 ± 0.22 [1.56, 1.68] r 0.327*	1,263.4 ± 182.0 1.54 ± 0.19 [1.49, 1.60] 0.325*	1,244.9 ± 169.2 1.52 ± 0.18 [1.48, 1.57] 0.353*
Upward (F <sub>z</sub> )	Combined (min)	658.4 ± 92.1 0.80 ± 0.08 [0.78, 0.82] r -0.231	658.8 ± 95.3 0.80 ± 0.07 [0.78, 0.82] -0.284*	668.0 ± 95.2 0.82 ± 0.07 [0.80, 0.83] -0.288*
	Lead	917.7 ± 213.4 1.12 ± 0.22 [1.06, 1.18] r 0.327*	940.9 ± 178.2 1.14 ± 0.19 [1.10, 1.20] 0.357*	951.8 ± 167.2 1.16 ± 0.17 [1.11, 1.21] 0.441*
	Trail	651.4 ± 105.1 0.79 ± 0.09 [0.77, 0.82] r 0.026	646.3 ± 100.0 0.79 ± 0.08 [0.77, 0.81] 0.113 (n = 62)	646.1 ± 96.8 0.79 ± 0.08 [0.77, 0.81] 0.121

\*Significantly ( $p < 0.05$ ) correlated to clubhead speed ( $n = 63$ ). In case outliers were identified, the actual sample size is provided. Ninety-five per cent CI of the M are provided. Correlation coefficients ( $r$ ) are between the peak normalised forces and the peak normalised clubhead speed. Magnitudes of the peak parameters were used in the correlation analysis. Peak vertical force parameters are all positive (upward). See Figure 5 for the generalised force patterns.

Table 2. Peak golfer–ground interaction moments (M ± SD [95% CI]) and their correlations to peak clubhead speed.

Variable	Foot	Club		
		Driver	5-Iron	Pitching wedge
GRF moment, F/B axis (G <sub>x</sub> )	Combined	137.8 ± 29.3	133.2 ± 27.3	124.7 ± 25.7
		16.79 ± 3.47 [15.92, 17.72]	16.18 ± 2.99 [15.45, 17.04]	15.20 ± 2.90 [14.45, 16.05]
		0.249*	0.220	0.346*
	Lead	157.7 ± 33.0	139.1 ± 27.2	127.2 ± 26.2
Pivoting moment (P <sub>2</sub> )		19.37 ± 3.26 [18.44, 20.08]	17.09 ± 2.73 [16.27, 17.70]	15.60 ± 2.66 [14.84, 16.26]
		0.319*	0.317*	0.448*
	Combined	106.4 ± 14.1	87.1 ± 12.5	75.4 ± 12.3
		13.12 ± 1.75 [12.56, 13.50]	10.76 ± 1.65 [10.24, 11.12]	9.32 ± 1.62 [8.83, 9.69]
		0.433*	0.421*	0.532*
	Lead	53.3 ± 14.4	42.5 ± 10.8	35.9 ± 9.0
		6.62 ± 1.80 [6.05, 7.00]	5.29 ± 1.34 [4.86, 5.56]	4.46 ± 1.18 [4.12, 4.73]
		-0.054	0.094	0.226
	Trail	60.7 ± 13.3	51.6 ± 10.5	46.2 ± 10.2
		7.43 ± 1.67 [6.97, 7.86]	6.32 ± 1.30 [5.97, 6.65]	5.64 ± 1.23 [5.32, 5.98]
		0.562*	0.518*	0.616*

\*Significantly ( $p < 0.05$ ) correlated to clubhead speed.

Ninety-five per cent CI of the M are provided. Correlation coefficients are between the peak normalised moments and the peak normalised clubhead speed. Peak moment parameters are all positive (counterclockwise), accelerating the downswing motion. See Figure 6 for the generalised moment patterns. F/B: forward/backward.

conditions (Table 2). No significant correlation was observed in the lead-foot pivoting moment. While most of the significant correlations were moderate, peak trail-foot pivoting moments showed large correlations.

When examined for each foot, the lead foot was characterised by significant correlations in the GRF moment about the F/B axis and all force components. The trail foot revealed significant correlations in the pivoting moment and forward force (Tables 1 and 2).

## Discussion and practical implications

The generalised patterns of the GRF components (Figure 5) highlight several important linear golfer-ground interaction aspects. The F/B components of the lead and trail foot show fairly symmetric force patterns throughout the entire swing (Williams, 2004), although the lead-foot backward GRF (caused by the forward push against the ground) is slightly larger than the trail-foot forward GRF (caused by the backward push against the ground) in the middle of the downswing (Figure 5(a)). As the F/B forces are fairly balanced throughout the entire swing, the motion of the CM of the body in the F/B direction should be minimal. The F/B GRFs reach their peak values near EDA, and both the lead-foot (backward) and trail-foot (forward) peak forces revealed significant correlations to maximum clubhead speed in all club conditions. In a group of 24 golfers (0–36 handicap), a significant correlation ( $r = 0.69$ ) between peak lead-foot backward force and maximum clubhead speed was previously reported (Williams, 2004). Previously reported F/B peak forces (Barrentine et al., 1994; Williams, 2004) were either comparable to or smaller than those observed in this study (Table 3).

The vertical forces also show symmetric patterns about the 0.5 BW line in the backswing and in the early phase of downswing with a larger force observed in the trail foot (Figure 5(c)). This caused the combined CP to shift towards the trail foot initially, and then shift back towards the centre in the backswing. The combined CP, however, remained closer to the trail foot at TB. The lead-foot vertical force got substantially larger in magnitude when compared to its counterpart in the downswing. As a result, the combined CP shifted quickly towards the lead foot during the TB-EDA phase. The combined vertical force pattern displayed an unweighing phase (vertical force < BW) in the late backswing phase and in the early part of downswing before the primary thrust occurred in the downswing. This essentially highlights the countermovement action used in the vertical direction. Both the unweighing peak (minimum vertical force) and the thrust peak (maximum vertical force) revealed significant correlations to clubhead speed in 2 or more club conditions (see Table 1). The unweighing peak was characterised by consistent negative correlations across club conditions; therefore, more unweighing was associated with higher clubhead speed. The thrust peak occurred midway between ED and MD, later than the F/B peaks. Previously reported peak vertical force values (Barrentine et al., 1994; Okuda et al., 2010) were fairly comparable to those observed in this study (see Table 3). Worsfold et al. (2007), however, reported much smaller average lead-foot and trail-foot vertical forces of 0.84 and 0.49 BW, respectively, for the driver condition.

Table 3. Comparison of the average peak ground reaction force values reported.

Study	<i>n</i>	Handicap	Mass (kg) CH speed (m/s)	Club	Forward/backward			Toward/away			Upward	
					Lead	Trail		Lead	Trail		Lead	Trail
Barrentine et al. (1994)	60 M	Pro, 0–15, 16+	86.7 ± 13.3	D	186 N	145 N		133 N	126 N		951 N	703 N
Chu et al. (2010)	266 M/42 F	8.4 ± 8.4	39.3 ± 2.7	5	162 N	129 N		123 N	128 N		964 N	695 N
			83.5 ± 17.0	D	-	-		-	-		0.95 BW <sup>a</sup>	0.41 BW <sup>a</sup>
Okuda et al. (2010)	11 M/2 F	0.8 ± 2.6	81.4 ± 10.7	D	-	-		-	-		1.09 BW	0.98 BW
Worsfold et al. (2007)	24 M	0–7, 8–14, 15+	75.3 ± 9.1	D	-	-		-	-		0.84 BW	0.49 BW
Williams (2004)	8 (24 M/4 F) <sup>b</sup>	0–8	42.0 ± 2.3	D	-	-		-	-		1.13–1.14 BW	0.82 BW
					-	-		-	-		1.07–1.19 BW	0.77–0.82 BW
					0.28 BW ( <i>r</i> = 0.69)*	-		-	-( <i>r</i> = 0.39)*		-	-
Current study	63 M	≤3	83.6 ± 8.8 48.3 ± 2.5	D	230 N	166 N		144 N	144 N		918 N	651 N
					0.28 BW*	0.21 BW*		0.18 BW*	0.18 BW		1.12 BW	0.79 BW
				5	210 N	154 N		126 N	134 N		941 N	646 N
					0.26 BW*	0.19 BW*		0.15 BW*	0.17 BW		1.14 BW	0.79 BW
				PW	192 N	147 N		119 N	127 N		952 N	646 N
					0.24 BW*	0.18 BW*		0.14 BW*	0.16 BW		1.16 BW	0.79 BW

<sup>a</sup>Values measured at 40 ms prior to impact.

<sup>b</sup>Number of participants used in the correlation analysis.

\*Significantly correlated (*p* < 0.05) to maximum clubhead speed.

M: male; F: female; CH: clubhead; D: driver; 3: 3-iron; 5: 5-iron; 7: 7-iron; PW: pitching wedge; BW: body weight.

The T/A forces exhibit smaller ranges than the other components with no symmetry observed (Figure 5(b)). The T/A forces were mostly inward, with the lead-foot force generally pushing the body away from the target, but the trail foot pushing towards (Williams, 2004). Overall, the combined T/A force was characterised by a longer towards push phase (before MB to ED). Between BA and MB, the CM of the body accelerated away, and then decelerated. From MB to ED, the CM accelerated towards the target, and then decelerated after ED. The body CM began shifting towards the target before the backswing was completed after the initial shift away. Due to the imbalance between the lead-foot and trail-foot T/A forces, the CM of the golfer-body system should have moved more in the T/A direction than in the F/B direction. The combined T/A force changed direction earlier than both the GRF moment about the F/B axis and the pivoting moment (Figure 6), which suggests a ‘shift-rotate-shift-rotate’ motion pattern (i.e., shift away → rotate back → shift towards → rotate down) in regards to the translation in the T/A direction and the rotation of the body during the swing. Barrentine et al. (1994) reported comparable peak T/A peak forces (Table 3). Williams (2004) reported a significant correlation between the trail-foot away peak and the maximum clubhead speed (Table 3).

One unique aspect of this study was the breakdown of the total external moment acting on the golfer-club system into moments representing different mechanisms: GRF moment, pivoting moment and foot contact moment. The GRF moment is the moment generated by the GRFs that can be explained by the combined GRF. The pivoting moment is the moment generated by individual GRFs about the combined CP and thus cannot be explained by the combined GRF acting at the combined CP (Equation (2)). The foot contact moment is due to the direct torsional interaction between the foot and the ground. From the generalised moment patterns (Figure 6(a,b)), the GRF moment about the F/B axis and the pivoting moment were identified as the primary moment terms. The other moment terms did not significantly contribute to angular momentum generation in the early phase of downswing due to small magnitudes (GRF moment about the vertical axis and foot contact moment) or late onset of the peak moment near BI (GRF moment about the T/A axis). With an inclined functional swing plane aligned closely towards the target (Kwon et al., 2012), the F/B axis and the vertical axis become the main axes of rotation. It is clear from the moment profiles that highly skilled male golfers generate the rotations about the F/B axis and the vertical axis by using the GRF moment mechanism and the pivoting moment mechanism, respectively.

The majority of the GRF moment about the F/B axis was derived from the lead foot (Figure 6(a)), as the lead-foot GRF vector formed a long moment arm against the body CM near EDA ( $d_L$  in Figure 2(a)) due to substantial loading on the lead foot. This moment arm must be sensitive to the T/A component of the lead-foot GRF ( $F_{y_L}$  in Figure 2(a)), as it forms a long moment arm about the CM (i.e., the height of the CM). The line of action of the trail-foot GRF at this position, in contrast, remained close to the body CM. The magnitude of the trail-foot GRF moment about the F/B axis therefore became small and the direction was typically opposite to that of the lead-foot moment (Figure 2(a)). The trail foot, however, was characterised by a greater contribution to the pivoting moment (Figure 6(b)).

The pivoting moment was primarily generated by the F/B GRFs of the feet, as the lines of action of the T/A GRFs stayed close to the combined CP (Figure 2(b)).

Although the magnitude of the trail-foot forward GRF was smaller than that of the lead-foot backward GRF near EDA (Figure 5(a)), the trail-foot pivoting moment arm must be much longer due to a much larger vertical GRF acting on the lead foot at this point (Figures 2(b) and 5(c)). The trail foot thus generated a larger pivoting moment, utilising a longer moment arm.

In summary, it appears that the primary angular role of the lead foot is to generate a large GRF moment about the F/B axis, while that of the trail foot is to generate a large pivoting moment about the vertical axis. Peak lead-foot GRF moment about the F/B axis and peak trail-foot pivoting moment yielded significant correlations to peak club-head speed. It should be noted that a substantial loading onto the lead foot near EDA (Figure 5(c)) was critical in generating both peak moments.

In Figure 6, both the GRF moment about the F/B axis and the pivoting moment exhibit negative values (causing acceleration of the backswing motion) in the early phase of backswing, but become positive after LB (causing deceleration of the backswing motion) while the backswing motion is still in progress until TB. As a result, large positive moment values are observed at the beginning of the downswing (TB), implying a countermovement-like role of the backswing motion. More specifically, the active deceleration of the backswing motion was immediately followed by acceleration of the downswing motion.

The contact moment is much smaller than the pivoting moment, with its ensemble maximum approximately 19% of the pivoting moment (Figure 6(b)). The magnitude of the contact moment decreases as the downswing motion progresses, and the ensemble contact-to-pivoting-moment ratio at the instant of the peak pivoting moment is only 9%. Although the GRMs (foot contact moments) acting on the feet could be meaningful in evaluating the shoe-ground interaction characteristics (Worsfold et al., 2008), its role in the golfer-ground interaction during the downswing is minimal.

Among the downswing events, EDA was identified as the point of maximum angular effort as both the F/B axis GRF moment and the pivoting moment reach their respective peak values slightly before or near this event (Figure 6). The GRF, in contrast, reaches its maximum magnitude midway between ED and MD (Figure 5), where the moments exhibit large decreases when compared to the peak values. It is clear from this temporal profile that: (1) the peak GRF moment about the F/B axis is not derived from the maximum GRF, and (2) the moment arm plays an important role in maximising the GRF moment about the F/B axis. Since a golf club is fairly long and its CM is located towards the head, the club's moment of inertia about the body CM can be large. To generate a high clubhead speed, it is necessary to (1) generate large golfer-ground interaction moments early in the downswing, (2) angularly accelerate the body sufficiently in the early phase of downswing, while maintaining the position of the club close to the body and (3) allow sufficient time for the club to accelerate in the later part of downswing through a delayed release of the club. This early onset of peak moments appears to be an important factor for the early development of body angular momentum and promotion of subsequent momentum transfer from the central body to arms/club.

In this study, only the peak golfer-ground interaction forces and moments were considered in the correlation analysis. While this approach allows for a big-picture understanding of the effects of linear and angular golfer-ground interactions on



clubhead speed, a more detailed study using an event-by-event approach (Ball & Best, 2007a; Chu et al., 2010; Okuda et al., 2010) is warranted, as even highly skilled golfers exhibit substantially different CM/CP shift patterns during the swing. The moment arm formed by the GRF with respect to the CM can be influenced greatly by the golfer's CM/CP shift patterns. The correlation profiles of the forces and moments at various meaningful swing instants (events) therefore will allow for a more in-depth understanding of the golfer-ground interaction. In addition, identification of distinct interaction styles based on methods, such as cluster analysis (Ball & Best, 2007a), and subsequent inter-style comparisons of various kinematic and kinetic parameters will allow investigators to assess whether specific interaction styles are superior to others in generating a high clubhead speed.

## Conclusion

The purpose of this study was to characterise the linear and angular golfer-ground interactions, and to identify meaningful associations between the peak golfer-ground interaction force and moment parameters and peak clubhead speed. For this, generalised patterns of key golfer-ground interaction force and moment components were established, and a correlation analysis was conducted between a group of select peak force and moment parameters and the clubhead speed. From the data analysis, it was concluded that:


- In highly skilled male golfers (handicap  $\leq 3$ ), the peak lead-foot GRFs were significantly correlated to maximum clubhead speed in all  $\beta$  directions (backward, away and upward). The peak trail-foot GRFs were significantly correlated to maximum clubhead speed in the forward direction only. Larger forces were associated with higher clubhead speed.
- The GRF moment about the F/B axis and the pivoting moment about the vertical axis were identified as the primary moment terms, and their peak moments (combined and lead-foot GRF moments about the F/B axis and combined and trail-foot pivoting moments) were significantly correlated to maximum clubhead speed, with larger moments associated with higher clubhead speed.
- The GRF moment about the F/B axis was primarily derived from the lead foot. The moment arm formed by the lead foot GRF with respect to the body CM plays a crucial role in this GRF moment mechanism. The trail foot contributed to the pivoting moment more than its counterpart did. The peak forward and backward GRFs of the feet play a key role in maximising the pivoting moment.
- A 'shift-rotate-shift-rotate' motion pattern (shift away  $\rightarrow$  rotate back  $\rightarrow$  shift towards  $\rightarrow$  rotate down) was evidenced by the combined T/A force's changing direction earlier than both the GRF moment about the F/B axis and the pivoting moment.
- The instant where the lead arm becomes parallel to the ground during the downswing was identified as the point of maximal angular effort, and the substantial loading onto the lead foot near this instant in the downswing is important in maximising the moments.



## Disclosure statement

AQ1 No potential conflict of interest was reported by the authors.

## References

- AQ2 Ball, K. A., & Best, R. J. (2007a). Different centre of pressure patterns within the golf stroke I: Cluster analysis. *Journal of Sports Sciences*, 25, 757–770. doi:10.1080/02640410600874971
- Ball, K. A., & Best, R. J. (2007b). Different centre of pressure patterns within the golf stroke II: Group-based analysis. *Journal of Sports Sciences*, 25, 771–779. doi:10.1080/02640410600875002
- Barrentine, S. W., Fleisig, G. S., Johnson, H., & Woolley, T. W. (1994). Ground reaction forces and torques of professional and amateur golfers. In A. J. Cochran & F. M. R. (Eds.), *Science and Golf II. Proceedings of the World Scientific Congress of Golf* (pp. 33–39). London: E & FN Spon.
- Chu, Y., Sell, T. C., & Lephart, S. M. (2010). The relationship between biomechanical variables and driving performance during the golf swing. *Journal of Sports Sciences*, 28, 1251–1259. doi:10.1080/02640414.2010.507249
- AQ3 De Leva, P. (1996). Adjustments to Zatsiorsky-Seluyanov's segment inertia parameters. *Journal of Biomechanics*, 29, 1223–1230.
- Hay, J. G. (1993). *The biomechanics of sports techniques* (4th ed.). Englewood Cliffs, NJ: Prentice Hall.
- Hellstrom, J. (2009). Competitive golf: A review of the relationships between playing results, technique and physique. *Sports Medicine*, 39, 723–741. doi:10.2165/11315200-000000000-00000
- Kwon, Y.-H. (2008). Measurement for deriving kinematic parameters: Numerical methods. In Y. Hong & R. M. Bartlett (Eds.), *Routledge handbook of biomechanics and human movement science* (pp. 156–181). Oxfordshire, UK: Routledge.
- Kwon, Y.-H., Como, C. S., Han, K., Lee, S., & Singhal, K. (2012). Assessment of planarity of the golf swing based on the functional swing plane of the clubhead and motion planes of the body points. *Sports Biomechanics*, 11, 127–148. doi:10.1080/14763141.2012.660799
- Kwon, Y.-H., Han, K. H., Como, C. S., Lee, S., & Singhal, K. (2013). Validity of the X-factor computation methods and relationship between the X-factor parameters and clubhead velocity in skilled golfers. *Sports Biomechanics*, 12, 231–246. doi:10.1080/14763141.2013.771896
- Lee, D. K. (2016). Alternatives to P value: Confidence interval and effect size. *Korean Journal of Anesthesiology*, 69, 555–562. doi:10.4097/kjae.2016.69.6.555
- AQ4  Okuda, I., Gribble, P., & Armstrong, C. (2010). Trunk rotation and weight transfer patterns between skilled and low skilled golfers. *Journal of Sports Science and Medicine*, 9, 127–133.
- Robinson, R. L. (1994). A study of the correlation between swing characteristics and club head velocity. In A. J. Cochran & M. R. Farrallay (Eds.), *Science and Golf II: Proceedings of the World Scientific Congress of Golf* (pp. 84–90). London: E & FN Span.
- AQ5 Williams, K. R. (2004). Relationships between ground reaction forces during the golf swing and ability level. *Engineering of Sport*, 1, 189–195.
- Williams, K. R., & Sih, B. L. (2002). Changes in golf clubface orientation following impact with the ball. *Sports Engineering*, 5, 65–80. doi:10.1046/j.1460-2687.2002.00093.x
- Winter, D. A. (2005). *Biomechanics and motor control of human movement* (3rd ed.). Hoboken, NJ: John Wiley & Sons.
- AQ6 Worsfold, P., Smith, N. A., & Dyson, R. J. (2007). A comparison of golf shoe designs highlights greater ground reaction forces with shorter irons. *Journal of Sports Science and Medicine*, 6, 484–489.
- AQ7 Worsfold, P., Smith, N. A., & Dyson, R. J. (2008). Low handicap golfers generate more torque at the shoe-natural grass interface when using a driver. *Journal of Sports Science and Medicine*, 7, 408–414.
- AQ8 Worsfold, P., Smith, N. A., & Dyson, R. J. (2009). Kinetic assessment of golf shoe outer sole design features. *Journal of Sports Science and Medicine*, 8, 607–615.
- AQ9 Zatsiorsky, V., & Seluyanov, V. (1983). The mass and inertia characteristics of the main segments of the human body. In H. Matsui & K. Kobayashi (Eds.), *Biomechanics* (Vols. VIII-B, pp. 1152–1159). Human Kinetics.